



Syddansk Universitet

Polarizable embedding with a multiconfiguration short-range density functional theory linear response method

Hedegård, Erik D.; Olsen, Jógvan Magnus Haugaard; Knecht, Stefan; Kongsted, Jacob; Jensen, Hans Jørgen Aagaard

Published in:
Journal of Chemical Physics

DOI:
[10.1063/1.4914922](https://doi.org/10.1063/1.4914922)

Publication date:
2015

Document version
Final published version

Citation for published version (APA):
Hedegård, E. D., Olsen, J. M. H., Knecht, S., Kongsted, J., & Jensen, H. J. A. (2015). Polarizable embedding with a multiconfiguration short-range density functional theory linear response method. *Journal of Chemical Physics*, 142, [1141113]. DOI: 10.1063/1.4914922

General rights

Copyright and moral rights for the publications made accessible in the public portal are retained by the authors and/or other copyright owners and it is a condition of accessing publications that users recognise and abide by the legal requirements associated with these rights.

- Users may download and print one copy of any publication from the public portal for the purpose of private study or research.
- You may not further distribute the material or use it for any profit-making activity or commercial gain
- You may freely distribute the URL identifying the publication in the public portal ?

Take down policy

If you believe that this document breaches copyright please contact us providing details, and we will remove access to the work immediately and investigate your claim.

Polarizable embedding with a multiconfiguration short-range density functional theory linear response method

Erik Donovan Hedegård, Jógvan Magnus Haugaard Olsen, Stefan Knecht, Jacob Kongsted, and Hans Jørgen Aagaard Jensen

Citation: *The Journal of Chemical Physics* **142**, 114113 (2015); doi: 10.1063/1.4914922

View online: <http://dx.doi.org/10.1063/1.4914922>

View Table of Contents: <http://scitation.aip.org/content/aip/journal/jcp/142/11?ver=pdfcov>

Published by the [AIP Publishing](#)

Articles you may be interested in

Excitation energies with linear response density matrix functional theory along the dissociation coordinate of an electron-pair bond in N-electron systems

J. Chem. Phys. **140**, 024101 (2014); 10.1063/1.4852195

Two-component relativistic density functional method for computing nonsingular complex linear response of molecules based on the zeroth order regular approximation

J. Chem. Phys. **130**, 194102 (2009); 10.1063/1.3123765

Density functional self-consistent quantum mechanics/molecular mechanics theory for linear and nonlinear molecular properties: Applications to solvated water and formaldehyde

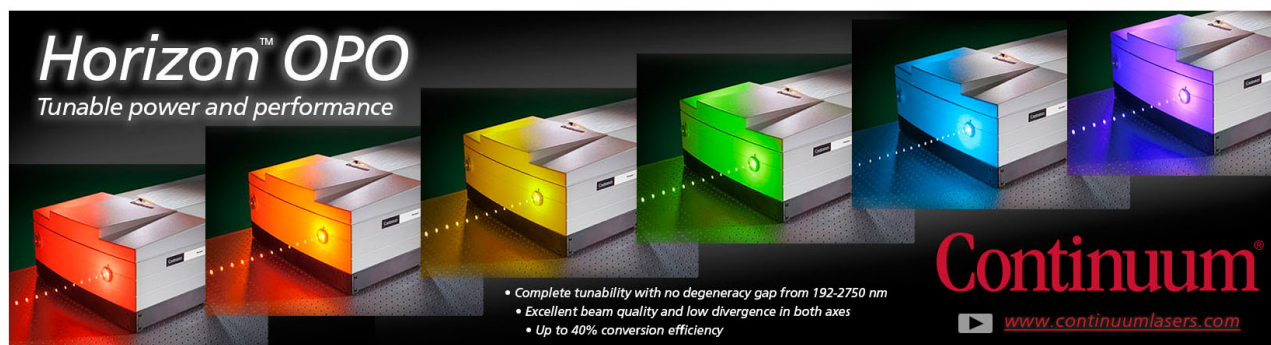
J. Chem. Phys. **126**, 154112 (2007); 10.1063/1.2711182

Resonance Raman spectra of uracil based on Kramers–Kronig relations using time-dependent density functional calculations and multireference perturbation theory

J. Chem. Phys. **120**, 11564 (2004); 10.1063/1.1697371

Density functional theory based effective fragment potential method

J. Chem. Phys. **118**, 6725 (2003); 10.1063/1.1559912



Horizon™ OPO
Tunable power and performance

• Complete tunability with no degeneracy gap from 192-2750 nm
• Excellent beam quality and low divergence in both axes
• Up to 40% conversion efficiency

Continuum®
www.continuumlasers.com

Polarizable embedding with a multiconfiguration short-range density functional theory linear response method

Erik Donovan Hedegård,^{1,2,a)} Jógvan Magnus Haugaard Olsen,^{3,2} Stefan Knecht,¹ Jacob Kongsted,^{2,b)} and Hans Jørgen Aagaard Jensen^{2,c)}

¹Laboratorium für Physikalische Chemie, ETH Zürich, Vladimir Prelog Weg 2, CH-8093 Zürich, Switzerland

²Department of Physics, Chemistry and Pharmacy, University of Southern Denmark, Campusvej 55, DK-5230 Odense, Denmark

³Laboratory of Computational Chemistry and Biochemistry, Ecole Polytechnique Fédérale de Lausanne, CH-1015 Lausanne, Switzerland

(Received 16 January 2015; accepted 3 March 2015; published online 19 March 2015)

We present here the coupling of a polarizable embedding (PE) model to the recently developed multiconfiguration short-range density functional theory method (MC-srDFT), which can treat multiconfigurational systems with a simultaneous account for dynamical and static correlation effects. PE-MC-srDFT is designed to combine efficient treatment of complicated electronic structures with inclusion of effects from the surrounding environment. The environmental effects encompass classical electrostatic interactions as well as polarization of both the quantum region and the environment. Using response theory, molecular properties such as excitation energies and oscillator strengths can be obtained. The PE-MC-srDFT method and the additional terms required for linear response have been implemented in a development version of DALTON. To benchmark the PE-MC-srDFT approach against the literature data, we have investigated the low-lying electronic excitations of acetone and uracil, both immersed in water solution. The PE-MC-srDFT results are consistent and accurate, both in terms of the calculated solvent shift and, unlike regular PE-MCSCF, also with respect to the individual absolute excitation energies. To demonstrate the capabilities of PE-MC-srDFT, we also investigated the retinylidene Schiff base chromophore embedded in the channelrhodopsin protein. While using a much more compact reference wave function in terms of active space, our PE-MC-srDFT approach yields excitation energies comparable in quality to CASSCF/CASPT2 benchmarks. © 2015 AIP Publishing LLC. [<http://dx.doi.org/10.1063/1.4914922>]

I. INTRODUCTION

Quantum mechanical methods have today a prominent place in chemical science, also in many experimental studies. Especially, the introduction of Kohn-Sham (KS) density functional theory (DFT) has revolutionized the role of computational and theoretical chemistry¹ due to its fast and often reliable performance for a large variety of properties.^{2,3} However, for systems with a degenerate or near-degenerate electronic ground state, the applicability of DFT is to some extent questionable, since a correct description requires a genuine multiconfigurational *ansatz*.^{4,5} Such systems are frequently encountered in biologically relevant molecules, for example, carotenoids^{6,7} and many transition metal enzymes.⁸ Another type of shortcomings occurs for the description of electronic excitations of doubly excited character (for exceptions, see Refs. 9 and 10) as well as excitations of charge-transfer (CT) type.^{11–15} Double excitations cannot be handled within the adiabatic linear-response formalism of time-dependent DFT, while CT excitations are severely underestimated due to the wrong long-range asymptotic behavior in the approximate DFT functional. For CT excitations, one strategy has been

range separation where the amount of exact Hartree-Fock exchange is varied with the inter-electronic distance, r_{12} .^{16–20}

The concept of range separation has also been exploited^{21–26} to develop hybrid theories between DFT and wave function theories. The developments presented in the following are based on the time-dependent formulation²⁷ of the multiconfiguration short-range DFT²⁸ (MC-srDFT) approach. This method capitalizes on the efficient treatment of the (short-range) Coulomb correlation within DFT and the ability of the multiconfiguration self-consistent field (MCSCF) method to recover large parts of the static correlation. It furthermore provides a wave function *ansatz* which can inherently handle molecules with low-lying double excitations. For molecular excitation energies, the aim of the MC-srDFT method is thus to be applicable for systems that are problematic with DFT, while still be at least of the same quality as DFT when DFT works reliably. This was recently investigated by some of us, and we verified that MC-srDFT is capable of yielding excitation energies for CT excitations with an accuracy competitive with CAM-B3LYP.²⁹ Very pleasing, excitations with extensive double excitation character were obtained at an accuracy comparable to CASPT2 for the retinylidene Schiff base chromophore, which is the active part of rhodopsin proteins.²⁹

However, these calculations were performed for molecules in gas-phase. Typically, chemistry takes place in

^{a)}Electronic mail: erik.hedegard@phys.chem.ethz.ch

^{b)}Electronic mail: kongsted@sdu.dk

^{c)}Electronic mail: hjj@sdu.dk

solution or inside a structured environment, e.g., a protein. Effects from such environments could be taken partly into account using continuum solvent models³⁰ although protein environments are problematic to describe by a structure-less continuum model. Approaches that consider the surrounding environment explicitly are more general. The most common explicit methods are hybrid quantum mechanics and molecular mechanics (QM/MM) methods.^{31,32} The standard molecular mechanics force fields that are typically used in QM/MM methods are nevertheless still crude, and energy contributions such as environment polarization are often ignored. Even standard polarizable force fields^{33,34} including an electrostatic component to describe polarization are often not sufficiently accurate to be applied in calculations of electronic properties. A more accurate approach is to calculate the embedding potential from first principles. This is done in the polarizable embedding (PE) model developed by Kongsted and coworkers.^{35–41} Here, the environment is described through distributed multipole moments and polarizabilities derived from *ab initio* calculations. This is to some extent similar in spirit to the effective fragment potential method.^{42–47} Further, the PE model considers not only the polarization between the quantum region and the classical environment but also the mutual polarization of the different sites *within* the environment. In this paper, we present the coupling of the PE model with the MC-srDFT method, to be denoted PE-MC-srDFT. The method is also extended to molecular properties through the corresponding linear response equations.

The paper is organized as follows: in Sec. II, we summarize the working equations for the MC-srDFT method and elaborate on the working equations for the new PE-MC-srDFT method. Also the time-dependent formulation of PE-MC-srDFT is discussed within the framework of linear response. Computational details are briefly summarized in Sec. III. In Sec. IV, we first present benchmark case studies where we compare excitation energies of solvated acetone and uracil to available literature data. Finally, we investigate the performance of the PE-MC-srDFT approach for the two lowest excited states of the retinylidene Schiff base chromophore embedded in a channelrhodopsin. A similar system has been investigated with the CASPT2 method.⁴⁸ Concluding remarks are then given in Sec. V.

II. THEORY

Our starting point here is the time-independent, vacuum electronic Hamiltonian, \hat{H}_0 , which in second quantization⁴⁹ is defined as

$$\hat{H}_0 = \sum_{pq} h_{pq} \hat{E}_{pq} + \sum_{pqrs} g_{pqrs} \hat{e}_{pqrs}, \quad (1)$$

where $\hat{E}_{pq} = \sum_{\sigma} \hat{a}_{p\sigma}^{\dagger} \hat{a}_{q\sigma}$ is the singlet one-electron operator, comprised of creation and annihilation operators, and $\hat{e}_{pqrs} = \hat{E}_{pq} \hat{E}_{rs} - \hat{E}_{ps} \hat{E}_{qr}$. The one- and two-electron integrals are contained in h_{pq} and g_{pqrs} ,

$$h_{pq} = \langle \phi_p | h(1) | \phi_q \rangle, \quad (2)$$

$$g_{pqrs} = \langle \phi_p(\mathbf{r}_1) \phi_r(\mathbf{r}_2) | g(1,2) | \phi_q(\mathbf{r}_1) \phi_s(\mathbf{r}_2) \rangle, \quad (3)$$

where $h(1)$ contains the one-electron terms for kinetic energy and nuclear-electron repulsion, and $g(1,2)$ is given as

$$g(1,2) = \frac{1}{|\mathbf{r}_1 - \mathbf{r}_2|}. \quad (4)$$

Although the MC-srDFT method has appeared in the literature,^{24,27,28} it has not emerged in a form which allows direct comparison to the second quantized DFT formalism.^{50,51} Thus, we summarize the second-quantized DFT and MC-srDFT methods in a form that highlights the similarities of the methods (Sec. II A). The equations that form the basis for the PE-MC-srDFT wave function optimization will be given in Sec. II B. In Sec. II C we present the corresponding linear response equations and the specific equations used in the implementation.

A. Multiconfiguration short-range DFT

The Kohn-Sham formulation of DFT uses a single determinant, $|0\rangle$, built from the Kohn-Sham orbitals $\{\phi_i\}$. These orbitals are used to construct the Kohn-Sham operator, defined as

$$\hat{f}_0 = \sum_{pq} f_{pq} \hat{E}_{pq}, \quad (5)$$

$$f_{pq} = h_{pq} + \mathcal{L}_{pq} + v_{xc,pq}.$$

We are generally using a closed-shell formulation and f_{pq} contains the integrals in Eq. (2) and also the integrals

$$\mathcal{L}_{pq} = \sum_{rs} g_{pqrs} D_{rs} - \frac{c_{\text{HF}}}{2} \sum_{rs} g_{psrq} D_{rs}, \quad (6)$$

$$v_{xc,pq} = \langle \phi_p | \hat{v}_{xc}(\mathbf{r}) | \phi_q \rangle,$$

where g_{pqrs} was defined in Eq. (3), c_{HF} is the amount of exact Hartree-Fock exchange ($0 \leq c_{\text{HF}} \leq 1$), and D_{rs} is a density matrix element,

$$D_{rs} = \langle 0 | \hat{E}_{rs} | 0 \rangle. \quad (7)$$

The $v_{xc}(\mathbf{r})$ term is the exchange-correlation potential and is formally defined as⁵¹

$$v_{xc}(\mathbf{r}) = \frac{\delta E_{xc}[\rho]}{\delta \rho(\mathbf{r})}, \quad (8)$$

and the exchange-correlation energy, $E_{xc}[\rho]$, is usually split into correlation and exchange parts,

$$E_{xc}[\rho] = (1 - c_{\text{HF}}) E_x[\rho] + E_c[\rho]. \quad (9)$$

Following Refs. 50 and 51, the electron density, ρ , can be written

$$\rho(\mathbf{r}) = \langle 0 | \hat{\rho}(\mathbf{r}) | 0 \rangle = \sum_{pq} \Omega_{pq}(\mathbf{r}) D_{pq}, \quad (10)$$

with $\Omega_{pq}(\mathbf{r}) = \phi_p^*(\mathbf{r}) \phi_q(\mathbf{r})$ and where $\hat{\rho}$ is the electron density operator,

$$\hat{\rho}(\mathbf{r}) = \sum_{pq} \Omega_{pq}(\mathbf{r}) \hat{E}_{pq}. \quad (11)$$

With the basic Kohn-Sham operators defined, we can now proceed to define the multi-configurational extension of DFT. The MC-srDFT method considered in this work relies on the

range separation of the regular two-electron repulsion^{22,24,27–29} term

$$g(1,2) \rightarrow g^{\text{lr},\mu}(1,2) + g^{\text{sr},\mu}(1,2). \quad (12)$$

The long-range and short-range interactions are based on the error function,

$$g^{\text{lr},\mu}(1,2) = \frac{\text{erf}(\mu|\mathbf{r}_1 - \mathbf{r}_2|)}{|\mathbf{r}_1 - \mathbf{r}_2|}, \quad (13)$$

$$g^{\text{sr},\mu}(1,2) = \frac{1 - \text{erf}(\mu|\mathbf{r}_1 - \mathbf{r}_2|)}{|\mathbf{r}_1 - \mathbf{r}_2|},$$

and μ is the range separation parameter. The partitioning in Eq. (13) gives rise to a new density-dependent long-range Hamiltonian

$$\hat{H}_0^\mu[\rho^\mu] = \sum_{pq} (h_{pq} + v_{\text{Hxc},pq}^\mu) \hat{E}_{pq} + \sum_{pqrs} g_{pqrs}^{\text{lr},\mu} \hat{e}_{pqrs}, \quad (14)$$

with

$$v_{\text{Hxc},pq}^\mu = \mathcal{L}_{pq}^\mu + v_{\text{xc},pq}^{\text{sr}}. \quad (15)$$

The evaluation of Eq. (15) thus corresponds to Eqs. (6) and (10) with the formal substitutions

$$g_{pqrs} \rightarrow g_{pqrs}^{\text{sr},\mu}, \quad (16)$$

$$v_{\text{xc},pq} \rightarrow v_{\text{xc},pq}^{\text{sr}},$$

$$D_{pq} \rightarrow D_{pq}^\mu = \langle 0^\mu | \hat{E}_{pq} | 0^\mu \rangle.$$

The $g_{pqrs}^{\text{sr},\mu}$ integrals are defined as Eq. (3), but with $g(1,2) \rightarrow g^{\text{sr},\mu}(1,2)$. $|0^\mu\rangle$ is a generalization of the Kohn-Sham determinant to a multiconfigurational wave function. The wave function *ansatz*, $|0^\mu\rangle$, used in this work reads

$$|0^\mu\rangle = e^{-\hat{\kappa}} \left(\frac{|0^\mu\rangle + \mathcal{P}|\mathbf{c}^\mu\rangle}{\sqrt{1 + \langle \mathbf{c}^\mu | \mathcal{P} | \mathbf{c}^\mu \rangle}} \right). \quad (17)$$

$\hat{\mathcal{P}} = 1 - |0^\mu\rangle\langle 0^\mu|$ is a projection operator and $\hat{\kappa}$ is the usual singlet orbital-rotation operator,

$$\hat{\kappa} = \sum_{pq} \kappa_{pq} (\hat{E}_{pq} - \hat{E}_{qp}) = \kappa_{pq} \hat{E}_{pq}^-, \quad (18)$$

while

$$|\mathbf{c}^\mu\rangle = \sum_j c_j |j^\mu\rangle, \quad (19)$$

is a configuration correction.

Finally, we can also define the MC-srDFT electron density

$$\rho^\mu(\mathbf{r}) = \langle 0^\mu | \hat{\rho}(\mathbf{r}) | 0^\mu \rangle, \quad (20)$$

which equals the density of the physical fully interacting system. The $\hat{\rho}(\mathbf{r})$ operator was defined in Eq. (11).

B. MC-srDFT with polarizable embedding

The PE model within a regular DFT framework has been defined through the modified KS operator,^{35,36}

$$\hat{f} = \hat{f}_0 + \hat{v}_{\text{pe}}, \quad (21)$$

where \hat{f}_0 is the vacuum KS operator (see Eq. (5)). The effective one-electron operator,

$$\hat{v}_{\text{pe}} = \hat{v}^{\text{es}} + \hat{v}^{\text{pol}}, \quad (22)$$

includes electrostatic interactions and polarization from sites in the environment through \hat{v}^{es} and \hat{v}^{pol} , respectively. The electrostatic interactions are described using permanent multipole moments (see, e.g., Ref. 40) while the polarization operator becomes

$$\hat{v}^{\text{pol}} = -\langle 0 | \hat{\mathbf{F}}^\dagger | 0 \rangle \mathbf{R} \hat{\mathbf{F}}^e = -(\boldsymbol{\mu}^{\text{ind}})^T \hat{\mathbf{F}}^e. \quad (23)$$

Here, $\langle 0 | \hat{\mathbf{F}}^\dagger | 0 \rangle$ is a row vector which contains the total electric field at all the polarizable sites, and $\hat{\mathbf{F}}^e$ is the electronic electric field operator. The symmetric matrix \mathbf{R} is the *classical response matrix*,⁵²

$$\mathbf{R} = \begin{pmatrix} \alpha_{11}^{-1} & \cdots & -\mathbf{T}_{1S}^{(2)} \\ \vdots & \ddots & \vdots \\ -\mathbf{T}_{S1}^{(2)} & \cdots & \alpha_{SS}^{-1} \end{pmatrix}^{-1}, \quad (24)$$

where α_{ss}^{-1} are inverse anisotropic polarizabilities and $\mathbf{T}_{s's}^{(2)}$ are dipole-dipole interaction tensors. The indices s and s' refer to different polarizable sites, and S is the total number of polarizable sites.

Analogously to Eq. (21), the PE operator can be added to the vacuum MC-srDFT Hamiltonian *ansatz*. The PE-MC-srDFT Hamiltonian thus becomes

$$\hat{H}^\mu[\rho^\mu] = \hat{H}_0^\mu[\rho^\mu] + \hat{v}_{\text{pe}}^\mu. \quad (25)$$

The PE potential, \hat{v}_{pe} , will be modified in a MC-srDFT scheme through its dependence on the wave function. Formally, this modification is obtained by substituting $|0\rangle \rightarrow |0^\mu\rangle$ in Eq. (23). The introduction of \hat{v}_{pe}^μ in Eq. (25) gives rise to additional terms in the electronic gradient and direct-Hessian vectors

$$\mathbf{g}^\mu = \mathbf{g}_0^\mu + \mathbf{g}_{\text{pe}}^\mu, \quad (26)$$

$$\boldsymbol{\sigma}^\mu = \boldsymbol{\sigma}_0^\mu + \boldsymbol{\sigma}_{\text{pe}}^\mu, \quad (27)$$

where \mathbf{g}_0^μ and $\boldsymbol{\sigma}_0^\mu$ are the vacuum contributions (see Appendix A). The simple form as a sum of vacuum and PE contributions is result of that there is no direct coupling between the vacuum and PE terms in Eq. (25). Both vacuum and PE contributions bear great resemblance to the original MCSCF and PE-MCSCF methods, which are explained in detail in the literature.^{40,53–56} Thus, Eqs. (26) and (27) can be derived explicitly by following the derivation outlined in Ref. 40, using the MC-srDFT wave function $|0^\mu\rangle$ instead of the regular MCSCF wave function. Here, we only give the relevant contributions from the environment. For the gradient, the contributions from a polarizable environment are

$$g_{\text{pe},j}^{c,\mu} = 2(\langle 0^\mu | \hat{v}_{\text{pe}}^\mu | j^\mu \rangle - c_j \langle 0^\mu | \hat{v}_{\text{pe}}^\mu | 0^\mu \rangle), \quad (28)$$

$$g_{\text{pe},pq}^{o,\mu} = 2\langle 0^\mu | [\hat{E}_{pq}, \hat{v}_{\text{pe}}^\mu] | 0^\mu \rangle,$$

for the CI and orbital parts, respectively. The c_j coefficients are given in Eq. (19).

The $\boldsymbol{\sigma}_{\text{pe}}$ vector splits according to

$$\boldsymbol{\sigma}_{\text{pe}}^\mu = \boldsymbol{\sigma}_{\text{pe}}^{c,\mu} + \boldsymbol{\sigma}_{\text{pe}}^{o,\mu} = \begin{pmatrix} \mathbf{H}_{\text{pe}}^{cc,\mu} \\ \mathbf{H}_{\text{pe}}^{oc,\mu} \end{pmatrix} \mathbf{b}^c + \begin{pmatrix} \mathbf{H}_{\text{pe}}^{co,\mu} \\ \mathbf{H}_{\text{pe}}^{oo,\mu} \end{pmatrix} \mathbf{b}^o, \quad (29)$$

where \mathbf{b}^c and \mathbf{b}^o are configuration- and orbital trial-vectors, respectively. Following the derivation in Ref. 40, the direct evaluation of the Hessian is described through a set of effective

operators. To define these, the $|B^\mu\rangle$ state from Ref. 40 is first given in its MC-srDFT form,

$$|B^\mu\rangle = \sum_j b_j^c |j^\mu\rangle, \quad (30)$$

and the effective PE operators thus become

$$\begin{aligned} \hat{F}^c(b^c) &= -\langle 0^\mu | \hat{F}^c | B^\mu \rangle \mathbf{R} \hat{F}^c, \\ \hat{F}^o(b^o) &= -\langle 0^\mu | \hat{F}^o(b^o) | 0^\mu \rangle \mathbf{R} \hat{F}^o, \\ \tilde{v}_{\text{pe}}^\mu(b^o) &= \tilde{v}^{\text{es}}(b^o) - \langle 0^\mu | \hat{F} | 0^\mu \rangle \mathbf{R} \hat{F}^o(b^o), \end{aligned} \quad (31)$$

where $\tilde{v}^{\text{es}}(b^o)$ and $\tilde{F}^o(b^o)$ are one-index transformed operators (see Ref. 40). The effective operators in Eq. (31) are now used to describe the components of the σ -vector in Eq. (29) as follows:

$$\begin{aligned} (\mathbf{H}_{\text{pe}}^{c^c, \mu} \mathbf{b}^c)_j &= 4 \left(\langle j^\mu | \hat{F}^c(b^c) | 0^\mu \rangle - \langle 0^\mu | \hat{F}^c(b^c) | 0^\mu \rangle c_j \right) \\ &\quad - 2 \left(\langle j^\mu | \hat{v}_{\text{pe}}^\mu | B^\mu \rangle - \langle 0^\mu | \hat{v}_{\text{pe}}^\mu | 0^\mu \rangle b_j^c \right), \\ (\mathbf{H}_{\text{pe}}^{c^o, \mu} \mathbf{b}^o)_j &= 2 \left(\langle 0^\mu | \hat{F}^o(b^o) + \tilde{v}_{\text{pe}}^\mu(b^o) | j^\mu \rangle \right) \\ &\quad - 2 \langle 0^\mu | \hat{F}^o(b^o) | 0^\mu \rangle c_j, \end{aligned} \quad (32)$$

and

$$\begin{aligned} (\mathbf{H}_{\text{pe}}^{o^c, \mu} \mathbf{b}^c)_{pq} &= 2 \langle 0^\mu | [\hat{E}_{pq}^-, \hat{F}^c(b^c) + \hat{v}_{\text{pe}}^\mu] | 0^\mu \rangle, \\ (\mathbf{H}_{\text{pe}}^{o^o, \mu} \mathbf{b}^o)_{pq} &= \langle 0^\mu | [\hat{E}_{pq}^-, \hat{F}^o(b^o) + \tilde{v}_{\text{pe}}^\mu(b^o)] | 0^\mu \rangle \\ &\quad + \frac{1}{2} \sum_t \left(g_{\text{pe}, tp}^{o, \mu} b_{qt}^o - g_{\text{pe}, tq}^{o, \mu} b_{pt}^o \right), \end{aligned} \quad (33)$$

where $g_{\text{pe}, ij}^{o, \mu}$ are matrix elements from the orbital part of gradient (Eq. (28)) and \hat{E}_{pq}^- is defined in Eq. (18). The Eqs. (32) and (33) comprise along with the gradient in Eq. (28), all ingredients necessary for optimizing a MC-srDFT wave function with contributions from a polarizable environment. In Sec. II C, such an optimized wave function will be assumed available.

C. Linear response PE-MC-srDFT equations

In this section, the effect of a time-dependent perturbation is considered through response theory; the time-evolution of the expectation value of a given operator, \hat{A} , is given as⁵⁷

$$\begin{aligned} \langle \tilde{0}^\mu(t) | \hat{A} | \tilde{0}^\mu(t) \rangle &= \langle 0^\mu | \hat{A} | 0^\mu \rangle \\ &\quad + \int_{-\infty}^{\infty} \langle \langle \hat{A}; \hat{V}^\omega \rangle \rangle \exp(-i\omega t) d\omega + \dots, \end{aligned} \quad (34)$$

where $\langle \langle \hat{A}; \hat{V}^\omega \rangle \rangle$ is the linear response function. The time-dependent reference state, $|\tilde{0}^\mu(t)\rangle$, is determined from the time-dependent Schrödinger equation

$$\langle \tilde{0}^\mu(t) | \left(\hat{H}[\rho^\mu(t)] + \hat{V}(t) \right) | \tilde{0}^\mu(t) \rangle = \langle 0^\mu(t) | i \frac{\partial}{\partial t} | 0^\mu(t) \rangle, \quad (35)$$

where $\hat{H}[\rho^\mu(t)]$ is the time-dependent extension of Eq. (25),

$$\hat{H}[\rho^\mu(t)] = \hat{H}_0^\mu[\rho^\mu(t)] + \hat{v}_{\text{pe}}^\mu(t) \quad (36)$$

and $\hat{V}(t)$ is a time-dependent, periodic perturbation.

The long-range MCSCF wave function in its time-dependent form is defined as

$$|\tilde{0}^\mu(t)\rangle = e^{i\hat{\kappa}(t)} e^{i\hat{S}(t)} |0^\mu\rangle, \quad (37)$$

with the $\hat{\kappa}(t)$ and $\hat{S}(t)$ operators in Eq. (37) defined as

$$\begin{aligned} \hat{\kappa}(t) &= \sum_i \kappa_i(t) \hat{q}_i^\dagger + \kappa_i^*(t) \hat{q}_i, \\ \hat{S}(t) &= \sum_i S_i(t) \hat{R}_i^\dagger + S_i^*(t) \hat{R}_i, \end{aligned} \quad (38)$$

where the $\hat{R}_i^\dagger = |i\rangle\langle 0^\mu|$ is a state-transfer operator, and we have followed the notation given by Olsen and Jørgensen⁵⁷ for the orbital rotation operators, $\hat{q}_i^\dagger = \hat{E}_{pq}$ ($p > q$). In the following, the summation in Eq. (38) will be implicit.

The linear response equations can be obtained from the generalized Ehrenfest theorem. This is done explicitly for PE-MCSCF in Ref. 40, and for DFT and MCSCF in Refs. 51 and 58, and 57 and 59, respectively. As for the electronic gradient and Hessian, the PE-MC-srDFT linear response equations can be derived by following the derivation in Ref. 40, using the PE-MC-srDFT Hamiltonian in Eq. (25). The final response equations become (here, given in the frequency domain)

$$(\mathbf{E}^{[2]\mu} - \omega \mathbf{S}^{[2]\mu}) \Lambda(\omega) = i \mathbf{V}^{[1]\omega \mu}. \quad (39)$$

Since there is no direct coupling between the vacuum and PE terms in Eq. (25), the Hessian is a sum of vacuum and PE contributions

$$\mathbf{E}^{[2]\mu} = \mathbf{E}_{\text{vac}}^{[2]\mu} + \mathbf{E}_{\text{pe}}^{[2]\mu}. \quad (40)$$

The expression for the metric, $\mathbf{S}^{[2]\mu}$, and the vacuum terms, $\mathbf{E}_{\text{vac}}^{[2]\mu}$, can be found in the literature^{27,29} and are also given in Appendix B.

The $\mathbf{E}_{\text{pe}}^{[2]\mu}$ term in Eq. (40) is the new term needed for this work,

$$\mathbf{E}_{\text{pe}}^{[2], \mu} = \begin{bmatrix} \mathbf{A}_{\text{pe}}^\mu & \mathbf{B}_{\text{pe}}^\mu \\ (\mathbf{B}_{\text{pe}}^\mu)^* & (\mathbf{A}_{\text{pe}}^\mu)^* \end{bmatrix} + \mathbf{R}(\mathbf{D}_{\text{aux}}^{[1]\mu} \mathbf{E}_{\text{e}}^{[1]\mu}). \quad (41)$$

The first term on the right-hand side contains the electrostatic contribution (static) and the contribution from the ground-state polarization, both included in the \hat{v}_{pe} operator

$$\mathbf{A}_{\text{pe}}^\mu = \begin{bmatrix} \langle 0^\mu | [\hat{q}_i, [\hat{v}_{\text{pe}}^\mu, \hat{q}_j^\dagger]] | 0^\mu \rangle & \langle 0^\mu | [[\hat{q}_i, \hat{v}_{\text{pe}}^\mu], \hat{R}_j^\dagger] | 0^\mu \rangle \\ \langle 0^\mu | [\hat{R}_i, [\hat{v}_{\text{pe}}^\mu, \hat{q}_j^\dagger]] | 0^\mu \rangle & \langle 0^\mu | [\hat{R}_i, [\hat{v}_{\text{pe}}^\mu, \hat{R}_j^\dagger]] | 0^\mu \rangle \end{bmatrix}, \quad (42)$$

$$\mathbf{B}_{\text{pe}}^\mu = \begin{bmatrix} \langle 0^\mu | [\hat{q}_i, [\hat{v}_{\text{pe}}^\mu, \hat{q}_j]] | 0^\mu \rangle & \langle 0^\mu | [[\hat{v}_{\text{pe}}^\mu, \hat{q}_i], \hat{R}_j] | 0^\mu \rangle \\ \langle 0^\mu | [\hat{R}_i, [\hat{v}_{\text{pe}}^\mu, \hat{q}_j]] | 0^\mu \rangle & \langle 0^\mu | [\hat{R}_i, [\hat{v}_{\text{pe}}^\mu, \hat{R}_j]] | 0^\mu \rangle \end{bmatrix}. \quad (43)$$

The second term on the right-hand side in Eq. (41) accounts for the change in polarization in the environment upon excitation through the auxiliary density matrix

$$\mathbf{D}_{\text{aux}}^{[1]\mu} = (\langle 0^\mu | [\hat{q}_i, \hat{F}^e] | 0^\mu \rangle + \langle 0^\mu | [\hat{R}_i, \hat{F}^e] | 0^\mu \rangle), \quad (44)$$

and the gradient-like term

$$\mathbf{E}_{\text{e}}^{[1]\mu} = \begin{bmatrix} \langle 0^\mu | [\hat{q}_j, \hat{F}^e] | 0^\mu \rangle \\ \langle 0^\mu | [\hat{R}_j, \hat{F}^e] | 0^\mu \rangle \\ \langle 0^\mu | [\hat{q}_j^\dagger, \hat{F}^e] | 0^\mu \rangle \\ \langle 0^\mu | [\hat{R}_j^\dagger, \hat{F}^e] | 0^\mu \rangle \end{bmatrix}. \quad (45)$$

The linear response function thus equals

$$\langle \langle \hat{A}; \hat{V} \rangle \rangle_\omega = -\mathbf{A}^{[1]\mu \dagger} [\mathbf{E}^{[2]\mu} - \omega \mathbf{S}^{[2]\mu}]^{-1} \mathbf{V}^{[1]\mu}, \quad (46)$$

where the gradient property vector has elements given as

$$\mathbf{V}^{[1]\mu} = \int v(\mathbf{r})\rho^{[1]\mu}(\mathbf{r})d\mathbf{r}. \quad (47)$$

The density gradient, $\rho^{[1]\mu}$, is defined through the density operator in Eq. (11),

$$\rho^{[1]\mu} = \begin{pmatrix} \langle 0^\mu | [\hat{q}_i, \hat{\rho}(\mathbf{r})] | 0^\mu \rangle \\ \langle 0^\mu | [\hat{R}_i, \hat{\rho}(\mathbf{r})] | 0^\mu \rangle \\ \langle 0^\mu | [\hat{q}_i^\dagger, \hat{\rho}(\mathbf{r})] | 0^\mu \rangle \\ \langle 0^\mu | [\hat{R}_i^\dagger, \hat{\rho}(\mathbf{r})] | 0^\mu \rangle \end{pmatrix}. \quad (48)$$

Excitation energies can now be calculated at the PE-MC-srDFT level by solving iteratively,

$$(\mathbf{E}^{[2]\mu} - \omega \mathbf{S}^{[2]\mu})\Lambda(\omega) = 0, \quad (49)$$

and oscillator strengths are determined by using the iteratively obtained $\Lambda(\omega)$ on the property gradient vectors $\mathbf{V}^{[1]\mu}$ (cf. Eq. (47)).

As for the wave function optimization, the $\mathbf{E}_{\text{pe}}^{[2]\mu}$ matrix is not constructed explicitly, as this would limit the implementation to very small systems. Following the original DALTON⁶⁰ linear response implementation, the current implementation

rather constructs the vector $\mathbf{E}_{\text{pe}}^{[2]N}(\omega)$ through trial vectors $\mathbf{N}(\omega)$,

$$\mathbf{N}(\omega) = (\boldsymbol{\kappa}, \mathbf{S}, \boldsymbol{\kappa}^*, \mathbf{S}^*). \quad (50)$$

The required operators are the $\tilde{v}_{\text{pe}}^\mu$ operator in Eq. (31) along with the effective operators

$$\hat{F}^{[1]} = \hat{F}^c(S) + \hat{F}^o(\boldsymbol{\kappa}), \quad (51)$$

which is defined similar to the $\hat{F}^c(b^c)$ and $\hat{F}^o(b^o)$ operators in Eq. (31),

$$\begin{aligned} \hat{F}^c(S) &= -(\langle 0^L | \hat{F}^c | 0^\mu \rangle + \langle 0^\mu | \hat{F}^c | 0^R \rangle) \mathbf{R} \hat{F}^c, \\ \hat{F}^o(\boldsymbol{\kappa}) &= -\langle 0^\mu | \hat{F}^o(\boldsymbol{\kappa}) | 0^\mu \rangle \mathbf{R} \hat{F}^c. \end{aligned} \quad (52)$$

We have in Eq. (52) defined the states

$$\begin{aligned} |0^R\rangle &= \sum_{n \neq 0} S_n \hat{R}_n^\dagger |0^\mu\rangle, \\ \langle 0^L| &= \sum_{n \neq 0} \langle 0^\mu | \hat{R}_n S_n^*, \end{aligned} \quad (53)$$

by means of state-transfer operators. An explicit derivation of the form of the operators in Eq. (52) and $\mathbf{E}_{\text{pe}}^{[2]N}(\omega)$ is given in Ref. 40. Here, we only summarize the final expression

$$\mathbf{E}_{\text{pe}}^{[2]N}(\omega) = \begin{bmatrix} \langle 0^L | [\hat{q}_j, \hat{v}_{\text{pe}}] | 0^\mu \rangle + \langle 0^\mu | [\hat{q}_j, \hat{v}_{\text{pe}}] | 0^R \rangle \\ \langle 0^L | \hat{v}_{\text{pe}} | j^\mu \rangle \\ \langle 0^L | [\hat{q}_j^\dagger, \hat{v}_{\text{pe}}] | 0^\mu \rangle + \langle 0^\mu | [\hat{q}_j^\dagger, \hat{v}_{\text{pe}}] | 0^R \rangle \\ -\langle j^\mu | \hat{v}_{\text{pe}} | 0^R \rangle \end{bmatrix} - \begin{bmatrix} \langle 0^\mu | [\hat{q}_j, \tilde{v}_{\text{pe}}^\mu(\boldsymbol{\kappa}) + \hat{F}^{[1]}] | 0^\mu \rangle \\ \langle 0^\mu | \tilde{v}_{\text{pe}}^\mu(\boldsymbol{\kappa}) + \hat{F}^{[1]} | j^\mu \rangle \\ \langle 0^\mu | [\hat{q}_j^\dagger, \tilde{v}_{\text{pe}}^\mu(\boldsymbol{\kappa}) + \hat{F}^{[1]}] | 0^\mu \rangle \\ \langle j^\mu | \tilde{v}_{\text{pe}}^\mu(\boldsymbol{\kappa}) + \hat{F}^{[1]} | 0^\mu \rangle \end{bmatrix} - \begin{bmatrix} 0 \\ S_j \\ 0 \\ S_j^* \end{bmatrix} \langle 0^\mu | \hat{v}_{\text{pe}} | 0^\mu \rangle. \quad (54)$$

The construction of $\mathbf{E}_{\text{pe}}^{[2]N}(\omega)$ in Eq. (54) relies on the existing implementation of PE-MCSCF.⁴⁰ With its extension to MC-srDFT, it is thus possible to calculate (static) spectroscopic constants of systems with significant static correlation in complex environments. The dynamic correlation is included efficiently through a short-range DFT functional, and the spectroscopic constants are obtained through linear response theory. For the case of a molecular excitation, double excitations are accessible, unlike in regular Kohn-Sham DFT. The interaction of the molecule and polarizable environment is taken into account for the ground-state and also for excited states through the second term in Eq. (41).

III. COMPUTATIONAL DETAILS

All calculations were performed using a development version of the DALTON program.^{60,61} Contributions from the environment are provided by the PE library⁶² which acquires one-electron integrals from the GenInt library.^{63,64} MC-srDFT and the corresponding response calculations are performed with the spin-independent Goll-Werner-Stoll short-range functional²⁶ (srPBE). The long-range interacting reference wave functions for the PE-MC-srDFT calculations are of the Complete Active Space Self-Consistent Field (CASSCF) type which implies a full configuration interaction expansion for n electrons in m orbitals denoted as CAS(n,m).

For acetone, a CAS(2,2) wave function was used, while for uracil, we used a CAS(6,6) wave function. These CAS spaces include the valence π -electrons. The aug-cc-pVDZ⁶⁵ basis set was used for both molecules. The acetone and uracil geometries, MD snapshots, and embedding potentials were taken from previous studies,^{35,66,67} and comprised 120 snapshots for each system. All reported values from the condensed phase are averages over a series of snapshots. The retinylidene Schiff base chromophore and protein structure are taken from Ref. 68. It is originally based on a crystal structure of the channelrhodopsin chimera C1C2⁶⁹ which was resolved at 2.3 Å (PDB ID: 3UG9). Note that we discovered some distorted methyl groups in the structure taken from Ref. 68 which were corrected in the present case. However, the irregularities were located very far from the active chromophore and had no effect on the excitation energies within the given accuracy. New embedding potentials were created using a Python script that automates and parallelizes the generation of potentials for polarizable embedding calculations and will be released in the near future. The script uses the molecular fractionation with conjugate caps (MFCC) scheme⁷⁰ to fragment the protein and the procedure reported by Söderhjelm and Ryde⁴⁸ to derive the embedding potential parameters. For each fragment, a MOLCAS⁷¹ calculation is performed to obtain atom-centered permanent multipole moments and polarizabilities. The properties are subsequently localized using the LoProp method.⁷²

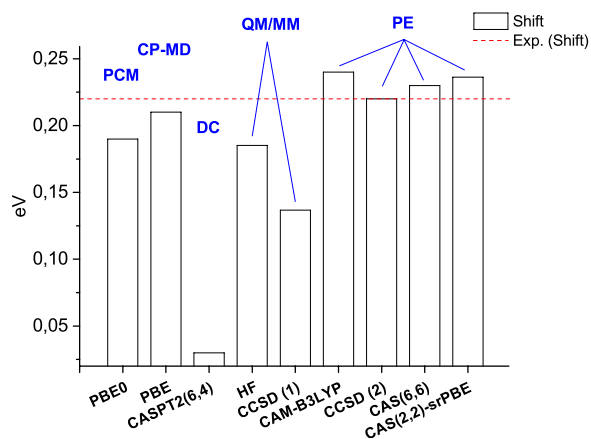


FIG. 1. Solvent shifts for the $n \rightarrow \pi^*$ excitation in acetone calculated with various methods. Data have been compiled from Refs. 35, 40, 66, and 74–81.

The fragment calculations were performed at the B3LYP level of theory using ANO-type reconstructions of the aug-cc-pVDZ basis set. We used a potential including multipoles up to quadrupoles and anisotropic dipole-dipole polarizabilities (“M2P2”). In addition, we also use a M2 potential which does not include polarizabilities. The retinylidene Schiff base was modeled using MC-srPBE with a CAS(6,6) active space and a 6-31G* basis set. The active space was chosen in accordance with previous studies.^{29,73}

IV. RESULTS AND DISCUSSION

In this section, we discuss the performance of the linear response PE-MC-srDFT method for the description of excitation energies and excited state properties in three representative molecular systems, namely, acetone in water (Sec. IV A), uracil in water (Sec. IV B), and the retinylidene Schiff base of a channelrhodopsin (Sec. IV C). Both the acetone and uracil solutions were recently investigated with regular MCSCF wave functions utilizing the same classical MD and potentials for the water environment.⁴⁰

A. Acetone

As the first test case for the new PE-MC-srDFT approach, we computed the low-lying excitation energies for acetone both in gas-phase and immersed in water. Acetone is a widely accepted guinea pig system for calculations on solute-solvent systems as reflected by the large amount of reference data available for this molecule. For acetone in aqueous solution, we recently found that the MCSCF/CASSCF *ansatz* performed remarkably well for the solvent shifts. We therefore start by discussing the solvent shift obtained with linear response PE-CAS(2,2)-srPBE. A comparison between excitation energies obtained with PE-CAS(6,6) and PE-CAS(2,2)-srPBE has been compiled in Figure 1, including also a selected series of the literature results. For acetone, all the polarizable embedding methods describe the solvent shift for the $n \rightarrow \pi^*$ excitation quite accurately. The most obvious outlier in Figure 2 is the CASPT2 method.⁷⁶ However, it should be emphasized that this is mainly due to the crude solvent description used in Ref. 76 and *not* due to shortcomings of the CASPT2 method itself. This will become evident from the quite accurate result for the gas-phase calculation obtained using CASPT2 discussed below. Although the first applications of the PE-MCSCF method have shown that it is able to yield good solvent shifts, it still significantly overestimates the absolute excitations. In Figure 2, the calculated solvent shifts for the $n \rightarrow \pi^*$ excitation in Figure 1 have been broken down to the absolute values of the gas-phase and condensed phase, respectively. From Figure 2, it can be seen that HF significantly underestimates the $n \rightarrow \pi^*$ excitation energy, while CASSCF significantly overestimates it. In both cases, it is thus a systematic error cancellation that eventually leads to reasonable solvent shifts. (PE)-CAS(2,2)-srPBE, on the other hand, gives consistent and accurate results, both in terms of the calculated solvent shift and for the individual (gas- and condensed phase) absolute excitation energies. Further comparison with the reference data in Figure 2 reveals that PE-CAS(2,2)-srPBE is comparable to PE-CCSD and PE-CAM-B3LYP, and thus a considerable improvement compared to regular PE-CAS. For the gas-phase results, we also note that CASPT2(4,6) and

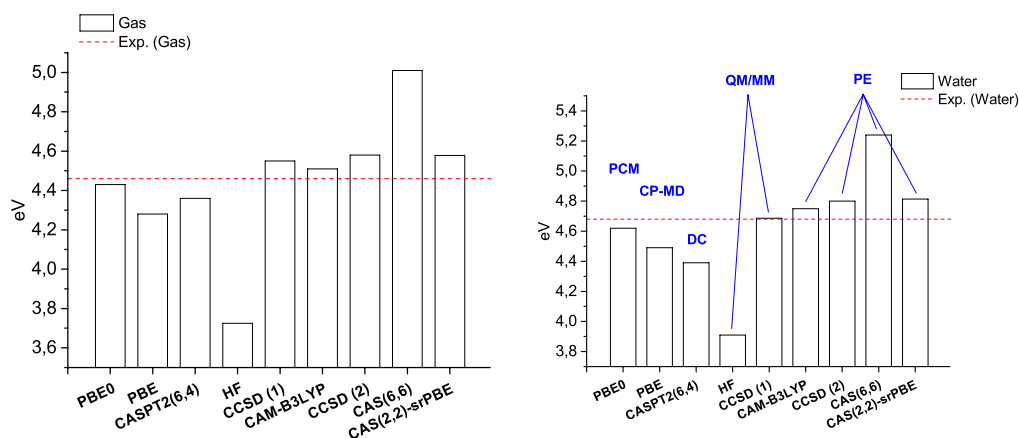


FIG. 2. $n \rightarrow \pi^*$ excitation for acetone calculated with various methods. Data have been compiled from Refs. 35, 40, 66, and 74–81 (the gas-phase results on the left-hand side are from the same references as the condensed phase data). CCSD(1) and CCSD(2) have slightly different computational setups, including the treatment of the water environment.

TABLE I. Vertical excitation energies (in eV) for uracil. CAS is shorthand for CAS(10,10), CB3 denotes CAM-B3LYP, and CAS-srPBE denotes CAS(6,6)-srPBE.

Environment	CAS ^a	CB3 ^a	CAS-srPBE	Expt. ^b
$\pi \rightarrow \pi^*$				
Gas phase	6.50	5.39	5.54	5.08
Water	6.24	5.27	5.38	4.77
Shift	-0.26	-0.12	-0.16	-0.31
$n \rightarrow \pi^*$				
Gas phase	6.14	5.05	5.12	4.38
Water	6.47	5.65	5.78	n.r.
Shift	0.32	0.60	0.66	...

^aFrom Ref. 40.^bExperimental values from Refs. 82–84. The $n \rightarrow \pi^*$ cannot be resolved in water.

CAS(2,2)-srPBE are roughly equally close to the experimental value, while the excitation energy in the condensed phase is significantly underestimated by CASPT2 with the applied dielectric continuum method (as also noted by the authors in Ref. 76).

B. Uracil

Our second test case is the nucleoside base uracil in aqueous solution. Uracil displays two low-lying excitations, which are closely spaced in energy. In gas-phase, the lowest lying excitation is of $n \rightarrow \pi^*$ type, followed by a $\pi \rightarrow \pi^*$ excitation. Theoretical data suggest that the two excitations interchange in aqueous solution (see discussion below). The absolute values for the excitation energies of the two electronic excitations calculated both in gas-phase and condensed phase are compiled in Table I along with the corresponding solvent shift. Table I summarizes in addition a few recent result obtained with PE in combination with other electronic structure methods. Starting with the $\pi \rightarrow \pi^*$ excitation, which has been experimentally resolved, the PE-MCSCF method (using a CAS(10,10) space⁴⁰) yields seemingly the most accurate solvent shift, while the shifts obtained for PE-CAS(6,6)-srPBE and PE-CAM-B3LYP are still reasonable. The results listed in Table I indicate the same pattern as seen as for acetone in Sec. IV A: Although (PE)-CAS gives quite accurate solvent *shifts*, the absolute excitations are off, both for the gas- and condensed phase, and the CASSCF approach greatly benefits from a favorable error cancellation. The improvements in the absolute $\pi \rightarrow \pi^*$ excitation energies are significant with the PE-CAS(6,6)-srPBE method. Turning next to the $n \rightarrow \pi^*$ excitation, PE-CAM-B3LYP and PE-CAS(6,6)-srPBE provide very similar results. No experimental data exist for this excitation in aqueous solution, but if we assume a similar accuracy to what is seen in the gas-phase, we can expect that the CASSCF results are also significantly off since CAS(6,6)-srPBE in the gas-phase is already much closer to the experimental result. However, with respect to the solvent shift, it is evident from the preceding discussion of the $\pi \rightarrow \pi^*$ excitation that this might still be obtained quite accurately by regular PE-CAS.

TABLE II. (PE-)CAS(6,6)-srPBE vertical excitation energies in eV (with oscillator strengths in parentheses) for the retinylidene Schiff base chromophore. The protein is included without (M2) or with explicit polarization (M2P2). All results are with 6-31G* basis set.

Environment	$S_0 \rightarrow S_1$ (1B_u)	$S_0 \rightarrow S_2$ (1A_g)
Gas-phase ²⁹	2.29 (1.60)	3.63 (0.52)
Protein (M2)	3.15 (1.98)	3.99 (0.25)
Protein (M2P2)	2.98 (2.06)	4.01 (0.25)
Expt. ⁸⁵	2.70	...

C. Channelrhodopsin

In order to test the PE-MC-srDFT method for a chromophore embedded within a protein, we selected channelrhodopsin, which has previously been studied with PE-CAM-B3LYP and PE-CC2.⁶⁸ Its active site is the retinylidene Schiff base chromophore which has recently also been subject to gas-phase MC-srDFT calculations²⁹ (using the structure from Ref. 68 that is optimized inside the protein). Here, we use the same structure that was employed in the previous studies.^{29,68} Results are compiled in Table II. The PE-CAS(6,6)-srPBE results obtained for the first transition $S_0 \rightarrow S_1$ (the bright state characterized by its considerably larger oscillator strength) are in good agreement with the PE-CAM-B3LYP and PE-CC2 values. Generally, looking at the results in Table II it becomes evident that the effect of the protein is crucial and that the effect from polarization from the environment is rather large and should not be neglected. The MC-srPBE method in combination with polarizable embedding is capable of describing the first ($S_0 \rightarrow S_1$) excitation with good accuracy compared to experiment. Although the basis set used is rather moderate, previous investigations have shown that this is not a major source of error. Thus, if higher accuracy is aimed for, one should also consider the quality of the underlying molecular structure or finite temperature effects. As discussed previously,²⁹ the dark state ($S_0 \rightarrow S_2$) originates from a double excitation that present-day TD-DFT approaches cannot describe. In contrast, this class of states can be described with MC-srPBE, and here, we have also probed the protein effect on the $S_0 \rightarrow S_2$ excitation. The effect of the protein is also for this transition, a rather large blue shift. However, polarization has a much smaller effect here than for the $S_0 \rightarrow S_1$ transition, in agreement with the fact that the second transition has much less CT character. It is evident from our results in Table II that to obtain the relative position of two excited states of a chromophore embedded in a protein, it is crucial to describe the environment accurately. We observe that the effect of the environment cannot only be very different but also depends on the nature of the excited states.

V. CONCLUSIONS

In this paper, we have presented the PE-MC-srDFT model in which the polarizable embedding model has been coupled to a hybrid scheme, namely, the multiconfiguration short-range DFT method. The PE-MC-srDFT method combines three elements in order to achieve our goal of efficient, yet

accurate description of large complex structures: “PE” for efficient description of the environment, “MC” for efficient description of static correlation, non-singlet spin states, and double excitations; and “srDFT” for efficient description of short-range dynamical correlation. The first part of the paper summarized the original vacuum MC-srDFT model. Following this subsection, the definition of the PE-MC-srDFT method was elaborated, and the working equations were derived. We then considered the generalization to time-dependent properties, giving the response equations and functions for the PE-MC-srDFT method. Although the linear response code is more general, the focus here is on excitation energies, and we have calculated solvent shifts and absolute excitation energies for two (explicitly) solvated systems and for a chromophore in a protein.

For both acetone and uracil, the absolute excitation energies show considerable improvement, both when compared to reference data from experiment and to high-level correlated wave function data.

As a final test case, we have considered a retinylidene chromophore in its Schiff base form surrounded by the native channelrhodopsin protein. The PE-MC-srPBE method describes the first ($S_0 \rightarrow S_1$) excitation accurately compared with experiment. We have also probed the effect of the protein on the dark state ($S_0 \rightarrow S_2$) that cannot be described with regular TD-DFT because it has significant double excitation character. For this excitation, the effect of the protein is also large and blue-shifts the excitation energy although polarization has a much smaller effect. The description of the environment is thus crucial to obtain a reasonable relative energy of two excited states for chromophores within proteins. A next obvious class of target systems is transition metals which are often found embedded in protein matrices. Also solvated transition metals are currently being studied with the PE-MC-srDFT method. Before closing, we note that the (PE)-MC-srDFT linear response code can also be used to calculate (frequency-dependent) polarizabilities, NMR shielding and spin-spin constants, and many other spectroscopic properties. This will be pursued in future work.

ACKNOWLEDGMENTS

E.D.H. thanks the Villum foundation for a post-doctoral fellowship. J.M.H.O. acknowledges financial support from the Danish Council for Independent Research through the Sapere Aude research career program. J.K. thanks the Villum and Lundbeck foundations as well as the Danish councils for independent research (Sapere Aude) for financial support. H.J.Aa.J. thanks the Danish Council for Independent Research | Natural Sciences for financial support (Grant No. 12-127074). The authors thank the Danish e-infrastructure cooperation for computational resources.

APPENDIX A: MC-SRDFT ELECTRONIC GRADIENT AND HESSIAN

This appendix recapitulates the equations required for MC-srDFT wave function optimization. The theoretical basis for the method has appeared in the literature before^{24,28} but

without explicit reference to the structure of the electronic gradient and Hessian.

The use of a multiconfigurational *ansatz* for the wave function $|0^\mu\rangle$ (see Eq. (17)) obviously necessitates a MCSCF optimization protocol. We utilize for this purpose the restricted step algorithm⁵³ implemented in DALTON. The restricted step algorithm is based on a second order Taylor expansion of the electronic energy, thus making use of both the gradient, \mathbf{g}^μ , and the electronic Hessian, \mathbf{H}^μ . The gradient,

$$\mathbf{g}_0^\mu = \begin{pmatrix} \mathbf{g}_0^{c,\mu} \\ \mathbf{g}_0^{o,\mu} \end{pmatrix}, \quad (\text{A1})$$

is comprised of configuration (\mathbf{g}_0^c) and orbital (\mathbf{g}_0^o) parts, respectively. The individual terms can be obtained as their MCSCF equivalents (e.g., taken from Refs. 53 and 54), using the $\hat{H}_0^\mu[\rho^\mu]$ operator in Eq. (14).

Turning to the Hessian, it is calculated in a direct manner,⁵⁴ utilizing a set of trial vectors $\{b_i\}$ ($\sigma = H_0 b$). The σ_0^μ vector can as the gradient be split into configuration and orbital parts,

$$\sigma_0^\mu = \begin{pmatrix} H_0^{cc,\mu} & H_0^{co,\mu} \\ H_0^{oc,\mu} & H_0^{oo,\mu} \end{pmatrix} \begin{pmatrix} b^c \\ b^o \end{pmatrix}, \quad (\text{A2})$$

or

$$\sigma_0^\mu = \sigma_0^{c,\mu} + \sigma_0^{o,\mu} = \begin{pmatrix} H_0^{cc,\mu} \\ H_0^{oc,\mu} \end{pmatrix} b^c + \begin{pmatrix} H_0^{co,\mu} \\ H_0^{oo,\mu} \end{pmatrix} b^o, \quad (\text{A3})$$

as in Eq. (29). The individual expressions have the same structure as the PE contributions in Eqs. (32) and (33)

$$\begin{aligned} (H_0^{cc,\mu} b^c)_j &= 4 \left(\langle j^\mu | \hat{v}_{\text{Hxc}}^{\text{eff},c}(b^c) | 0^\mu \rangle - \langle 0^\mu | \hat{v}_{\text{Hxc}}^{\text{eff},c}(b^c) | 0^\mu \rangle c_j \right) \\ &\quad - 2 \left(\langle j^\mu | \hat{H}_0^\mu[\rho^\mu] | B^\mu \rangle \right. \\ &\quad \left. - \langle 0^\mu | \hat{H}_0^\mu[\rho^\mu] | 0^\mu \rangle b_j^c \right), \end{aligned} \quad (\text{A4})$$

$$\begin{aligned} (H_0^{co,\mu} b^o)_j &= 2 \langle 0^\mu | \hat{v}_{\text{Hxc}}^{\text{eff},o} + \tilde{H}_0^\mu[\rho^\mu](b^o) | j^\mu \rangle \\ &\quad - 2 \langle 0^\mu | \hat{v}_{\text{Hxc}}^{\text{eff},o}(b^o) | 0^\mu \rangle c_j \end{aligned}$$

and

$$\begin{aligned} (H_0^{oc,\mu} b^c)_{pq} &= 2 \langle 0^\mu | [\hat{E}_{pq}^-, \hat{v}_{\text{Hxc}}^{\text{eff},c}(b^c) + \hat{H}_0^\mu[\rho^\mu]] | 0^\mu \rangle, \\ (H_0^{oo,\mu} b^o)_{pq} &= \langle 0^\mu | [\hat{E}_{pq}^-, \hat{v}_{\text{Hxc}}^{\text{eff},o}(b^o) + \tilde{H}_0^\mu[\rho^\mu](b^o)] | 0^\mu \rangle \\ &\quad + \frac{1}{2} \sum_t (g_{0,tp}^{o,\mu} b_{qt}^o - g_{0,tq}^{o,\mu} b_{pt}^o), \end{aligned} \quad (\text{A5})$$

where $\tilde{H}_0^\mu[\rho^\mu](b^o)$ is the one-index transformed form of $\hat{H}_0^\mu[\rho^\mu]$ (see Eq. (14)). The operators $\hat{v}_{\text{Hxc}}^{\text{eff},c}(b^c)$ and $\hat{v}_{\text{Hxc}}^{\text{eff},o}(b^o)$ are effective operators with slightly different forms, depending on whether they have origin in configuration ($\hat{v}_{\text{Hxc}}^{\text{eff},c}$) or orbital ($\hat{v}_{\text{Hxc}}^{\text{eff},o}$) parameters. Their forms are similar to the $\hat{F}^c(b^c)$ and $\hat{F}^o(b^o)$ operators in Eq. (31), but with origin in the DFT term. Explicit expressions have been given elsewhere.⁵⁶ The reason for the similarity between the PE and MC-srDFT effective operators is the underlying operator structure; for both PE-MCSCF and MC-srDFT, the additional operators that are introduced relative to standard MCSCF are one-electron operators of non-linear type.

APPENDIX B: LINEAR RESPONSE MC-SRDFT EQUATIONS

The linear response equations derived previously²⁷ are further recast in a form that enables the direct extension of the second quantized DFT formalism as given by Saue and Salek^{50,51} to a multiconfigurational formalism.

As done in previous papers on response theory,^{51,57,59} we use a perturbation expansions of Eq. (38),

$$\begin{aligned}\hat{\kappa}(t) &= \hat{\kappa}^{(1)}(t) + \hat{\kappa}^{(2)}(t) + \dots, \\ \hat{S}(t) &= \hat{S}^{(1)}(t) + \hat{S}^{(2)}(t) + \dots.\end{aligned}\quad (\text{B1})$$

Along the same lines as in Ref. 51, we expand the Hamiltonian in a perturbation series, which for the vacuum part (Eq. (14)) becomes

$$\hat{H}_0^\mu[\rho^\mu(t)] = \hat{H}_0^{(0)\mu}[\rho^\mu] + \hat{H}^{(1)\mu}[\rho^\mu(t)] + \dots \quad (\text{B2})$$

The auxiliary Hamiltonian, $\hat{H}_0^{(0)\mu}[\rho^\mu]$, is calculated for the unperturbed MC-srDFT density, $\rho^\mu(\mathbf{r})$, while the first order correction, $\hat{H}^{(1)\mu}[\rho^\mu(t)]$, depends on the MC-srDFT density gradient, $\rho^{(1)\mu}(\mathbf{r}, t)$, that is obtained from⁵¹

$$\begin{aligned}\rho^\mu(\mathbf{r}, t) &= \langle \tilde{0}^\mu(t) | \hat{\rho}(\mathbf{r}) | \tilde{0}^\mu(t) \rangle \\ &= \langle 0^\mu | e^{-i\hat{S}(t)} e^{-i\hat{\kappa}(t)} \hat{\rho}(\mathbf{r}) e^{i\hat{\kappa}(t)} e^{i\hat{S}(t)} | 0^\mu \rangle.\end{aligned}\quad (\text{B3})$$

A Baker-Campbell-Hausdorff expansion of Eq. (B3) yields to first order

$$\rho^{(1)\mu}(\mathbf{r}, t) = \sum_{pq} \Omega_{pq}(\mathbf{r}) D_{pq}^{(1)\mu}(t), \quad (\text{B4})$$

where the time-dependence to first order is obtained through the time-dependent density matrix

$$D_{pq}^{(1)\mu}(t) = \langle 0^\mu | [\hat{\kappa}^{(1)}(t) + \hat{S}^{(1)}(t), \hat{E}_{pq}] | 0^\mu \rangle. \quad (\text{B5})$$

$\hat{H}^{(1)\mu}[\rho^\mu(t)]$ thus becomes

$$\hat{H}^{(1)\mu}[\rho^\mu(t)] = \sum_{pq} v_{\text{Hxc}, pq}^{(1)\mu}(t) \hat{E}_{pq}, \quad (\text{B6})$$

$$v_{\text{Hxc}, pq}^{(1)\mu}(t) = \mathcal{L}_{pq}^{(1)\mu}(t) + v_{\text{xc}, pq}^{(1)\text{sr}}(t),$$

where $\hat{v}_{\text{Hxc}, pq}^{(1)\text{sr}}(t)$ is the first-order time-dependent extension of Eq. (15),

$$\begin{aligned}\mathcal{L}_{pq}^{(1)\mu}(t) &= \sum_{rs} g_{pqrs}^{\text{sr}, \mu} D_{rs}^{(1)\mu}(t) - \frac{c_{\text{HF}}}{2} \sum_{rs} g_{psrq}^{\text{sr}, \mu} D_{rs}^{(1)\mu}(t), \\ v_{\text{xc}, pq}^{(1)\text{sr}}(t) &= \langle \phi_p | v_{\text{xc}}^{(1)\text{sr}}(\mathbf{r}, t) | \phi_q \rangle.\end{aligned}\quad (\text{B7})$$

The exchange-correlation kernel is calculated using the adiabatic approximation

$$\begin{aligned}\hat{v}_{\text{xc}}^{(1)\text{sr}}(\mathbf{r}, t) &= \int d\mathbf{r}' \frac{\delta \hat{v}_{\text{xc}}^{\text{sr}}(\mathbf{r}, t)}{\delta \rho(\mathbf{r}')} \rho^{(1)\mu}(\mathbf{r}', t) \\ &\approx \int d\mathbf{r}' \frac{\delta^2 E_{\text{xc}}^{\text{sr}}[\rho^\mu]}{\delta \rho(\mathbf{r}) \delta \rho(\mathbf{r}')} \rho^{(1)\mu}(\mathbf{r}', t).\end{aligned}\quad (\text{B8})$$

Since the final response equations will be calculated in the frequency domain rather than the time-domain, the wave function coefficients are Fourier transformed,

$$\begin{aligned}\hat{\kappa}_i^{(1)}(t) &= \int (\kappa_i(\omega) \hat{q}_i^\dagger e^{-i\omega t} + \kappa_i^*(-\omega) \hat{q}_i e^{i\omega t}) d\omega, \\ \hat{S}_i^{(1)}(t) &= \int (S_i(\omega) \hat{R}_i^\dagger e^{-i\omega t} + S_i^*(-\omega) \hat{R}_i e^{i\omega t}) d\omega.\end{aligned}\quad (\text{B9})$$

In the frequency domain, the first-order density matrix in Eq. (B5) becomes

$$D_{pq}^{\omega\mu} = \begin{pmatrix} \kappa_j(\omega) & S_j(\omega) & \kappa_j^*(-\omega) & S_j^*(-\omega) \end{pmatrix} \begin{pmatrix} \langle 0^\mu | [\hat{q}_j, \hat{E}_{pq}] | 0^\mu \rangle \\ \langle 0^\mu | [\hat{R}_j, \hat{E}_{pq}] | 0^\mu \rangle \\ \langle 0^\mu | [\hat{q}_j^\dagger, \hat{E}_{pq}] | 0^\mu \rangle \\ \langle 0^\mu | [\hat{R}_j^\dagger, \hat{E}_{pq}] | 0^\mu \rangle \end{pmatrix} = \Lambda(\omega) D_{pq}^{[1]\mu}, \quad (\text{B10})$$

and the density gradient is thus transformed into

$$\rho^{\omega\mu} = \Lambda(\omega) \rho^{[1]\mu}, \quad (\text{B11})$$

where $\rho^{[1]\mu}$ was given in Eq. (48). With Eqs. (B10) and (B11), it is now possible to define the Fourier transformed $H^{(1)\mu}[\rho^\mu(t)]$ of Eq. (B6),

$$\begin{aligned}\hat{H}^{\omega\mu} &= H^{[1]\mu} \Lambda(\omega), \\ \hat{H}^{[1]\mu} &= \sum_{pq} v_{\text{Hxc}, pq}^{[1]\mu} \hat{E}_{pq} = \sum_{pq} (\mathcal{L}_{pq}^{[1]\mu} + v_{\text{xc}, pq}^{[1]\text{sr}}) \hat{E}_{pq},\end{aligned}\quad (\text{B12})$$

where the integrals $\mathcal{L}_{pq}^{[1]\mu}$ and $v_{\text{xc}, pq}^{[1]\text{sr}}$ are defined as in Eqs. (B7), with the replacements $D_{pq}^{(1)\mu} \rightarrow D_{pq}^{[1]\mu}$ and $\rho^{(1)\mu} \rightarrow \rho^{[1]\mu}$, i.e., Eqs. (B10) and (B11) are used instead of (B4) and (B5), respectively. The kernel is calculated using the unperturbed

MC-srDFT density,

$$v_{\text{xc}}^{[1]\mu}(\mathbf{r}) = \int d\mathbf{r}' \frac{\delta^2 E_{\text{xc}}^{\text{sr}}[\rho^\mu]}{\delta \rho(\mathbf{r}) \delta \rho(\mathbf{r}')} \rho^{[1]\mu}(\mathbf{r}'). \quad (\text{B13})$$

With all wave function parameters and perturbation expansions defined, the response equations can now be obtained from the generalized Ehrenfest theorem (as done in Refs. 57 and 59). To obtain the first order corrections, the expansion in Eqs. (B1) and (B6) is used and the resulting equation is transformed to the frequency domain, leading to Eq. (39) with

$$E_{\text{vac}}^{[2]\mu} = E_0^{[2]\mu} + E_{\text{Hxc}}^{[2]\mu}. \quad (\text{B14})$$

$E_0^{[2]\mu}$ and also the μ -dependent metric, $S^{[2]\mu}$, in Eq. (39),

$$E_0^{[2]\mu} = \begin{bmatrix} A^\mu & B^\mu \\ B^{\mu*} & A^{\mu*} \end{bmatrix}, \quad S^{[2]\mu} = \begin{bmatrix} \Sigma^\mu & \Delta^\mu \\ -\Delta^{\mu*} & -\Sigma^{\mu*} \end{bmatrix}, \quad (\text{B15})$$

are obtained as their regular MCSCF counterparts (see, e.g., Refs. 57 and 59), with $\hat{H}_0 \rightarrow \hat{H}_0^{[0]\mu}[\rho^\mu]$ and $|0\rangle \rightarrow |0^\mu\rangle$. The full form of these two matrices are given in recent MC-srDFT papers.^{27,29} The contribution from the srDFT part becomes

$$E_{\text{Hxc}}^{[2]\mu} = \begin{bmatrix} A_{\text{Hxc}}^\mu & B_{\text{Hxc}}^\mu \\ B_{\text{Hxc}}^{\mu*} & A_{\text{Hxc}}^{\mu*} \end{bmatrix}, \quad (\text{B16})$$

where

$$A_{\text{Hxc}}^\mu = \begin{bmatrix} \langle 0^\mu | [\hat{q}_i, (\hat{H}_j^{[1]\mu})^\dagger] | 0^\mu \rangle & \langle 0^\mu | [\hat{R}_i, (\hat{H}_j^{[1]\mu})^\dagger] | 0^\mu \rangle \\ \langle 0^\mu | [\hat{q}_i^\dagger, (\hat{H}_j^{[1]\mu})] | 0^\mu \rangle & \langle 0^\mu | [\hat{R}_i^\dagger, (\hat{H}_j^{[1]\mu})] | 0^\mu \rangle \end{bmatrix}, \quad (\text{B17})$$

$$B_{\text{Hxc}}^\mu = \begin{bmatrix} \langle 0^\mu | [\hat{q}_i^\dagger, (\hat{H}_j^{[1]\mu})^\dagger] | 0^\mu \rangle & \langle 0^\mu | [\hat{R}_i^\dagger, (\hat{H}_j^{[1]\mu})^\dagger] | 0^\mu \rangle \\ \langle 0^\mu | [\hat{q}_i, (\hat{H}_j^{[1]\mu})] | 0^\mu \rangle & \langle 0^\mu | [\hat{R}_i, (\hat{H}_j^{[1]\mu})] | 0^\mu \rangle \end{bmatrix}. \quad (\text{B18})$$

The $\hat{H}_j^{[1]\mu}$ term is given in Eq. (B12) and the j -index refers to the state-transfer or orbital-rotation operators used in evaluation of $D^{[1]}$ or $\rho^{[1]}$. The actual evaluation of $E_{\text{vac}}^{[2]\mu}$ uses a direct Hessian formulation similar to the electronic Hessian in Eqs. (A4) and (A5), also relying on effective operators.

- ¹K. Burke, *J. Chem. Phys.* **136**, 150901 (2012).
²M. A. L. Marques and E. K. U. Gross, *Annu. Rev. Phys. Chem.* **55**, 427 (2004).
³M. Casida and M. Huix-Rotllant, *Annu. Rev. Phys. Chem.* **63**, 287 (2012).
⁴V. Veryazov, P. Å. Malmqvist, and B. O. Roos, *Int. J. Quantum Chem.* **111**, 3329 (2011).
⁵P. G. Szalay, T. Müller, G. Gidofalvi, H. Lischka, and R. Shepard, *Chem. Rev.* **112**, 108 (2012).
⁶M. Kleinschmidt, C. M. Marian, M. Waletzke, and S. Grimme, *J. Chem. Phys.* **130**, 044708 (2009).
⁷A. Muñoz-Losa, M. E. Matfín, I. F. Galván, M. L. Sánchez, and M. A. Aguilar, *J. Chem. Theory Comput.* **7**, 4050 (2011).
⁸K. Pierloot, *Int. J. Quantum Chem.* **111**, 3291 (2011).
⁹N. T. Maitra, F. Zhang, R. J. Cave, and K. Burke, *J. Chem. Phys.* **120**, 5932 (2004).
¹⁰P. Elliot, S. Goldson, C. Canahui, and N. T. Maitra, *Chem. Phys.* **391**, 110 (2011).
¹¹D. J. Tozer, R. D. Amos, N. C. Handy, B. Roos, and L. Serrano-Andrés, *Mol. Phys.* **97**, 859 (1999).
¹²M.-S. Liao, Y. Lu, and S. Scheiner, *J. Comput. Chem.* **24**, 623 (2003).
¹³E. Fabiano, F. Della Sala, G. Barbarella, S. Lattante, M. Anni, G. Sotgiu, C. Hättig, R. Cingolani, and G. Gigli, *J. Phys. Chem. B* **110**, 18651 (2006).
¹⁴E. Perpète, J. Preat, J.-M. André, and D. Jacquemin, *J. Phys. Chem. A* **110**, 5629 (2006).
¹⁵A. Dreuw and M. Head-Gordon, *J. Am. Chem. Soc.* **126**, 4007 (2004).
¹⁶H. Iikura, T. Tsuneda, T. Yanai, and K. Hirao, *J. Chem. Phys.* **115**, 3540 (2001).
¹⁷T. Yanai, D. P. Tew, and N. C. Handy, *Chem. Phys. Lett.* **393**, 51 (2004).
¹⁸O. A. Vydrov and G. E. Scuseria, *J. Chem. Phys.* **125**, 234109 (2006).
¹⁹M. A. Rohrdanz, K. M. Martins, and J. M. Herbert, *J. Chem. Phys.* **130**, 054112 (2009).
²⁰R. Baer, E. Livshits, and U. Salzner, *Annu. Rev. Phys. Chem.* **61**, 85 (2010).
²¹A. Savin and H.-J. Flad, *Int. J. Quantum Chem.* **56**, 327 (1995).
²²A. Savin, *Recent Developments and Applications of Modern Density Functional Theory* (Elsevier, Amsterdam, 1996), p. 327.
²³J. G. Ángyán, I. C. Gerber, A. Savin, and J. Toulouse, *Phys. Rev. A* **72**, 012510 (2005).
²⁴E. Fromager and H. J. Aa. Jensen, *Phys. Rev. A* **78**, 022504 (2008).
²⁵E. Fromager, R. Cimraglia, and H. J. Aa. Jensen, *Phys. Rev. A* **81**, 024502 (2010).
²⁶E. Goll, H.-J. Werner, and H. Stoll, *Phys. Chem. Chem. Phys.* **7**, 3917 (2005).
²⁷E. Fromager, S. Knecht, and H. J. Aa. Jensen, *J. Chem. Phys.* **138**, 084101 (2013).
²⁸E. Fromager, J. Toulouse, and H. J. Aa. Jensen, *J. Chem. Phys.* **126**, 074111 (2007).
²⁹E. D. Hedegård, F. Heiden, S. Knecht, E. Fromager, and H. J. Aa. Jensen, *J. Chem. Phys.* **139**, 184308 (2013).
³⁰J. Tomasi, B. Mennucci, and R. Cammi, *Chem. Rev.* **105**, 2999 (2005).
³¹A. Warshel and M. Levitt, *J. Mol. Biol.* **103**, 227 (1976).
³²H. M. Senn and W. Thiel, *Angew. Chem., Int. Ed.* **48**, 1198 (2009).
³³W. L. Jorgensen, *J. Chem. Theory Comput.* **3**, 1877 (2007).
³⁴C. B. Nielsen, O. Christiansen, K. V. Mikkelsen, and J. Kongsted, *J. Chem. Phys.* **126**, 154112 (2007).
³⁵J. M. Olsen, K. Aidas, and J. Kongsted, *J. Chem. Theory Comput.* **6**, 3721 (2010).
³⁶J. M. H. Olsen and J. Kongsted, *Adv. Quantum Chem.* **61**, 107 (2011).
³⁷K. Sneskov, T. Schwabe, J. Kongsted, and O. Christiansen, *J. Chem. Phys.* **134**, 104108 (2011).
³⁸T. Schwabe, K. Sneskov, J. M. H. Olsen, J. Kongsted, O. Christiansen, and C. Hättig, *J. Chem. Theory Comput.* **8**, 3274 (2012).
³⁹N. H. List, H. J. Aa. Jensen, J. Kongsted, and E. D. Hedegård, *Adv. Quantum Chem.* **66**, 195 (2013).
⁴⁰E. D. Hedegård, N. H. List, H. J. Aa. Jensen, and J. Kongsted, *J. Chem. Phys.* **139**, 044101 (2013).
⁴¹M. N. Pedersen, E. D. Hedegård, J. M. H. Olsen, J. Kauczor, P. Norman, and J. Kongsted, *J. Chem. Theory Comput.* **10**, 1164 (2014).
⁴²P. N. Day, J. H. Jensen, M. S. Gordon, S. Webb, and W. J. Stevens, *J. Chem. Phys.* **105**, 1968 (1996).
⁴³M. S. Gordon, P. Feitag, M. A. Bandyopadhyay, J. H. Jensen, V. Kairys, and W. J. Stevens, *J. Phys. Chem. A* **105**, 293 (2001).
⁴⁴M. S. Gordon, L. V. Slipchenko, H. Li, and J. H. Jensen, *Annu. Rep. Comput. Chem.* **3**, 177 (2007).
⁴⁵S. Yoo, F. Zahariev, S. Sok, and M. S. Gordon, *J. Chem. Phys.* **129**, 144112 (2008).
⁴⁶P. Arora, L. V. Slipchenko, S. P. Webb, A. DeFusco, and M. S. Gordon, *J. Phys. Chem. A* **114**, 6742 (2010).
⁴⁷L. V. Slipchenko, *J. Phys. Chem. A* **114**, 8824 (2010).
⁴⁸P. Söderhjelm and U. Ryde, *J. Phys. Chem. A* **113**, 617 (2009).
⁴⁹T. Helgaker, P. Jørgensen, and J. Olsen, *Molecular Electronic Structure Theory* (Wiley, 2004).
⁵⁰T. Saue and T. Helgaker, *J. Comput. Chem.* **23**, 814 (2002).
⁵¹P. Salek, O. Vahtras, T. Helgaker, and H. Ågren, *J. Chem. Phys.* **117**, 9630 (2002).
⁵²J. Applequist, J. R. Carl, and K.-K. Fung, *J. Am. Chem. Soc.* **94**, 2952 (1972).
⁵³H. J. Aa. Jensen and P. Jørgensen, *J. Chem. Phys.* **80**, 1204 (1984).
⁵⁴H. J. Aa. Jensen and H. Ågren, *Chem. Phys.* **104**, 229 (1986).
⁵⁵H. J. Aa. Jensen, in *Relativistic and Electronic Correlation in Molecules and Solids*, edited by G. L. Malli (Plenum Press, 1994), pp. 179–206.
⁵⁶J. K. Pedersen, “Description of correlation and relativistic effects in calculations of molecular properties,” Ph.D. thesis (University of Southern Denmark, Odense, 2004).
⁵⁷J. Olsen and P. Jørgensen, *J. Chem. Phys.* **82**, 3235 (1985).
⁵⁸P. Salek, T. Helgaker, and T. Saue, *Chem. Phys.* **311**, 187 (2005).
⁵⁹J. Olsen and P. Jørgensen, in *Modern Electronic Structure Theory*, edited by D. R. Yarkony (World Scientific, 1995), Vol. 2, pp. 857–990.
⁶⁰K. Aidas, C. Angeli, K. L. Bak, V. Bakken, R. Bast, L. Boman, O. Christiansen, R. Cimraglia, S. Coriani, P. Dahle, E. K. Dalskov, U. Ekström, T. Enevoldsen, J. J. Eriksen, P. Ettenhuber, B. Fernández, L. Ferrighi, H. Fliegl, L. Frediani, K. Hald, A. Halkier, C. Hättig, H. Heiberg, T. Helgaker, A. C. Hennum, H. Hettema, E. Hjertenæs, S. Høst, I.-M. Høyvik, M. F. Iozzi, B. Jansik, H. J. Aa. Jensen, D. Jonsson, P. Jørgensen, J. Kauczor, S. Kirpekar, T. Kjergaard, W. Klopper, S. Knecht, R. Kobayashi, H. Koch, J. Kongsted, A. Krapp, K. Kristensen, A. Ligabue, O. B. Lutnæs, J. I. Melo, J. V. Mikkelsen, R. H. Myhre, C. Neiss, C. B. Nielsen, P. Norman, J. Olsen, K. M. H. Olsen, A. Osted, M. J. Packer, F. Pawłowski, T. B. Pedersen, P. F. Provasi, S. Reine, Z. Rinkevicius, T. A. Ruden, K. Ruud, V. V. Rybkin, P. Salek, C. C. M. Samson, A. S. de Merás, T. Saue, S. P. A. Sauer, B. Schimmelpfennig, K. Sneskov, A. H. Steindal, K. O. Sylvester-Hvid, P. R. Taylor, A. M. Teale, E. I. Tellgren, D. P. Tew, A. J. Thorvaldsen, L. Thøgersen, O. Vahtras, M. A. Watson, D. J. D. Wilson, M. Ziolkowski, and H. Ågren, *WIREs Comput. Mol. Sci.* **4**, 269 (2014).
⁶¹See <http://daltonprogram.org/> for DALTON, a molecular electronic structure program, development version.
⁶²J. M. H. Olsen, PELIB: The Polarizable Embedding library (version 1.0.8), 2014.
⁶³B. Gao, Gen1Int version 0.2.1, 2012, <http://repo.ctcc.no/projects/gen1int>.

- ⁶⁴B. Gao, A. J. Thorvaldsen, and K. Ruud, *Int. J. Quantum Chem.* **111**, 858 (2011).
- ⁶⁵T. H. Dunning, Jr., *J. Chem. Phys.* **90**, 1007 (1989).
- ⁶⁶K. Aidas, J. Kongsted, A. Osted, K. V. Mikkelsen, and O. Christiansen, *J. Phys. Chem. A* **109**, 8001 (2005).
- ⁶⁷J. M. Olsen, K. Aidas, K. V. Mikkelsen, and J. Kongsted, *J. Chem. Theory Comput.* **6**, 249 (2010).
- ⁶⁸K. Sneskov, J. M. H. Olsen, T. Schwabe, C. Hättig, O. Christiansen, and J. Kongsted, *Phys. Chem. Chem. Phys.* **15**, 7567 (2013).
- ⁶⁹H. E. Kato, F. Zhang, O. Yizhar, C. Ramakrishnan, T. Nishizawa, K. Hirata, J. Ito, Y. Aita, T. Tsukazaki, S. Hayashi, P. Hegemann, A. D. Maturana, R. Ishitani, K. Deisseroth, and O. Nureki, *Nature* **482**, 369 (2012).
- ⁷⁰D. W. Zhang and J. Z. H. Zhang, *J. Chem. Phys.* **119**, 3599 (2003).
- ⁷¹F. Aquilante, L. De Vico, G. Ferré, G. Ghigo, P.-Å. Malmqvist, P. Neogrády, T. B. Pedersen, M. Pitoňák, M. Reiher, B. O. Roos, L. Serrano-Andrés, M. Urban, V. Verayzov, and R. Lindh, *J. Comput. Chem.* **31**, 224 (2009).
- ⁷²L. Gagliardi, R. Lindh, and G. Karlström, *J. Chem. Phys.* **121**, 4494 (2004).
- ⁷³E. D. Hedegård, H. J. Aa. Jensen, and J. Kongsted, *Int. J. Quantum Chem.* **114**, 1102 (2014).
- ⁷⁴F. Aquilante, M. Cossi, O. Crescenzi, G. Scalmani, and V. Barone, *Mol. Phys.* **101**, 1945 (2003).
- ⁷⁵O. Crescenzi, M. Pavone, F. De Angelis, and V. Barone, *J. Phys. Chem. B* **109**, 4445 (2005).
- ⁷⁶L. Serrano-Andrés, M. P. Fülscher, and G. Karlström, *Int. J. Quantum Chem.* **65**, 167 (1997).
- ⁷⁷F. C. Grozema and P. T. van Duijnen, *J. Phys. Chem. A* **102**, 7984 (1998).
- ⁷⁸N. S. Bayliss and E. G. McRae, *J. Phys. Chem.* **58**, 1006 (1954).
- ⁷⁹W. P. Hayes and C. J. Timmons, *Spectrochim. Acta* **21**, 529 (1965).
- ⁸⁰N. S. Bayliss and G. Willis-Johnson, *Spectrochim. Acta* **24A**, 551 (1965).
- ⁸¹T. Schwabe, J. M. H. Olsen, K. Sneskov, J. Kongsted, and O. Christiansen, *J. Chem. Theory Comput.* **7**, 2209 (2011).
- ⁸²L. B. Clark, G. G. Peschel, and I. Tinoco, Jr., *J. Phys. Chem.* **69**, 3615 (1965).
- ⁸³M. Daniels and W. Hauswirth, *Science* **171**, 675 (1971).
- ⁸⁴M. Fujii, T. Tamura, N. Mikami, and M. Ito, *Chem. Phys. Lett.* **126**, 583 (1986).
- ⁸⁵E. Ritter, K. Stehfest, A. Berndt, P. Hegemann, and F. Bartl, *J. Biol. Chem.* **283**, 35033 (2008).